[Channels 1:2, 92-101; March/April 2007]; ©2007 Landes Bioscience

Research Paper

The HOOK-Domain Between the SH3 and the GK Domains of $Ca_v\beta$ Subunits Contains Key Determinants Controlling Calcium Channel Inactivation

Mark W. Richards[1,2]
Jerôme Leroy[1,3]
Wendy S. Pratt[1]
Annette C. Dolphin[1,*]

[1]Laboratory of Cellular and Molecular Neuroscience; Department of Pharmacology; University College London; London UK

[2]Present address: The Institute of Cancer Research; Chester Beatty Labs; London UK

[3]Present address: Inserm U446; Laboratoire de Cardiologie Cellulaire et Moleculaire; Faculté de Pharmacie; Université Paris Sud; Chatenay Malabry Cedex, France

[*]Correspondence to: Annette C. Dolphin; Laboratory of Cellular and Molecular Neuroscience; Department of Pharmacology; University College London; Gower Street; London WC1E 6BT UK; Tel.: 44.20.7679.0048; Fax: 44.20.7679.0042; Email: a.dolphin@ucl.ac.uk

Original manuscript submitted: 03/04/07
Revised manuscript submitted: 03/15/07
Manuscript accepted: 03/15/07

Previously published online as a *Channels* E-Publication:
http://www.landesbioscience.com/journals/channels/article/4145

KEY WORDS

calcium channel, β subunit, electrophysiology

ACKNOWLEDGEMENTS

This work was supported by The Wellcome Trust. We thank the following for generous gifts of cDNAs: Dr Y. Mori (Seriken, Okazaki, Japan) for rabbit $Ca_v2.2$; Dr E. Perez-Reyes (Loyola University, Chicago, IL) for rat β_{2a}; Dr. R. T. Hughes (Yale, New Haven, CT) for mut-3 GFP; Genetics Institute (Cambridge, MA) for pMT2. We also thank K. Chaggar for technical assistance and Selvan Bavan for performing some of the molecular biology.

ABSTRACT

$Ca_v\beta$ subunits of voltage-gated calcium channels contain two conserved domains, a *src*-homology-3 (SH3)-domain and a guanylate kinase-like (GK)-domain. The SH3-domain is split, with its final (fifth) β-strand separated from the rest of the domain by an intervening sequence termed the HOOK-domain, whose sequence varies between $Ca_v\beta$ subunits. Here we have been guided by the recent structural studies of $Ca_v\beta$ subunits in the design of specific truncated constructs, with the goal of investigating the role of the HOOK-domain of $Ca_v\beta$ subunits in the modulation of inactivation of N-type calcium channels. We have coexpressed the β subunit constructs with $Ca_v2.2$ and $\alpha_2\delta$-2, using the N-terminally palmitoylated β_{2a} subunit, because it supports very little voltage-dependent inactivation, and made comparisons with β_{1b} domains. Deletion of the variable region of the β_{2a} HOOK-domain resulted in currents with a rapidly inactivating component, and additional mutation of the β_{2a} palmitoylation motif further enhanced inactivation. The isolated GK-domain of β_{2a} alone enhanced current amplitude, but the currents were rapidly and completely inactivating. When the β_{2a}-GK-domain construct was extended proximally, by including the HOOK-domain and the ε-strand of the SH3-domain, inactivation was about four-fold slower than in the absence of the HOOK domain. When the SH3-domain of β_{2a} truncated prior to the HOOK-domain was coexpressed with the (HOOK+εSH3+GK)-domain of β_{2a}, all the properties of β_{2a} were restored, in terms of loss of inactivation. Furthermore, removal of the HOOK sequence from the (HOOK+εSH3+GK)-β_{2a} construct increased inactivation. Together, these results provide evidence that the HOOK domain is an important determinant of inactivation.

INTRODUCTION

Voltage-gated calcium (Ca_v) channels play a major role in the physiology of all excitable cells. Three families have been identified, Ca_v1-3 (reviewed in ref. 1). The high-voltage-activated (HVA) Ca_v1 and 2 classes are heteromultimers composed of the pore-forming α_1 subunit, associated with auxiliary $Ca_v\beta$ and $\alpha_2\delta$ subunits (reviewed in ref. 2). Four $Ca_v\beta$ subunit genes have been cloned, and these subunits are important for HVA channel function (reviewed in ref. 3), since they promote expression of functional channels at the plasma membrane and modulate their biophysical properties.[4-7] $Ca_v\beta$ subunits bind with high affinity to the α-interaction domain (AID) on the I-II loop of Ca_v1 and 2 channels,[4] although other α_1 subunit interaction sites are also likely to be important in mediating the actions of $Ca_v\beta$ subunits.[8,9]

In a previous study we investigated the role of $Ca_v\beta$ subunits in the plasma membrane expression and G-protein modulation of $Ca_v2.2$ calcium channels, by mutating the AID tryptophan (W391) in the I-II loop of $Ca_v2.2$, and thus completely disrupting the high affinity interaction with $Ca_v\beta$ subunits.[10] Our main conclusion was that, whereas the $Ca_v2.2$W391A mutant channels lost all modulation by β_{1b}, the same was not true for palmitoylated $Ca_v\beta_{2a}$. Only expression at the plasma membrane was affected when $Ca_v\beta_{2a}$ was coexpressed with the mutant $Ca_v2.2$W391A channel, while all the biophysical properties of the expressed $Ca_v2.2$W391A channels remained normally modulated by $Ca_v\beta_{2a}$, including the marked depolarization of steady-state inactivation, which is typical of palmitoylated $Ca_v\beta_{2a}$. We concluded that the continuing influence of β_{2a} was dependent on its palmitoylation, which increased the local concentration near the plasma membrane sufficiently to allow lower affinity interactions to occur between $Ca_v\beta$ and channel α_1 subunit, which were effective in modulating the channel properties.[10]

$Ca_v\beta$ subunits were predicted by structural modelling to contain an SH3-domain followed by a guanylate kinase (GK) domain.[11] X-ray crystallographic studies have

produced detailed information on the domain structure.[12-14] The N-terminal SH3-domain is divided, with its final (5th) β-strand, providing the interaction with the GK-domain, being situated after the variable HOOK region, whose structure was not determined (reviewed in ref. 15). We have been guided by the structure in our choice of truncations and deletions in the present study (Fig. 1A and B). In the case of the GK domains, we have used the exon boundary to determine the C-terminal end, since such boundaries often delimit a stable functional domain, and this marks the end of the second conserved domain, as originally identified (reviewed in ref. 16). It was important that the GK domain constructs were stable since previous studies have examined the properties of several GK-domain constructs with varying results, regarding their ability to mimic the functions of intact $Ca_v\beta$ subunits, which might have indicated varying stabilities in different cell types.[17,18] We have now dissected the role of the variable HOOK-domain, between the conserved SH3 and GK domains, and our results indicate that this region contains key determinants of both closed and open state calcium channel inactivation. Furthermore, it is likely that the extent of interaction of the channel with this HOOK region is determined by the palmitoylation state of the SH3-domain.

MATERIALS AND METHODS

Materials. The cDNAs used in this study were $Ca_v2.2$ (D14157), $Ca_v\beta_{1b}$ (X61394), $Ca_v\beta_{2a}$ (M88751) and $\alpha_2\delta$-2.[19] When used, the green fluorescent protein (GFP-mut3b, U73901) was used to identify transfected cells. All cDNAs were subcloned into pMT_2.

Construction of truncated β subunit domains. All constructs were made by standard molecular biological techniques and their sequences verified by sequencing both strands. The constructs used (with their amino acid residues) were β_{2a}-core (1-442), β_{2a} Δ-vHOOK (Δ 169-213), β_{2a} truncated SH3 (1-135), β_{2a}-(SH3+HOOK+εSH3) (1-225), β_{2a}-GK (226-442), β_{2a}-(HOOK+ εSH3+GK) (136-442), β_{2a}-(ΔHOOK+εSH3+GK) (214-442), β_{1b}-truncated-SH3 (82-178), β_{1b}-GK (230-426), β_{1b}-(HOOK+εSH3+GK) (179-426) and β_{1b}-(ΔHOOK+εSH3+GK) (217-426).

Two electrode voltage-clamp. *Xenopus* oocytes were prepared, injected and utilized for two electrode voltage clamp electrophysiology as previously described.[20] Briefly, plasmid cDNAs for the different VDCC subunits $Ca_v2.2$, $\alpha_2\delta$-2 and β subunit were mixed in weight ratios of 2:1:2 at 1 $\mu g.\mu l^{-1}$. When separate GK and SH3-domains were used, these cDNAs were mixed in a ratio of 2:1. The final DNA mix was diluted 3-fold and 9 nl injected intranuclearly into stage V or VI oocytes. Injected oocytes were incubated at 18°C for 3–4 days in ND96 saline plus 1.8 mM $CaCl_2$ supplemented with 50 IU/ml penicillin and 50 μg/ml streptomycin (Invitrogen, Paisley, UK). Recordings from oocytes were made in the two-electrode voltage clamp configuration, using a Geneclamp 500B and Digidata 1200 (Molecular Devices, Foster City, CA), with an extracellular chloride-free solution containing (in mM): $Ba(OH)_2$ 10; NaOH 70; CsOH 2; Hepes 5 (pH 7.4 with methanesulfonic acid). Oocytes were injected with 30–40 nl of a 100 mM solution of K_3-1,2-bis (amino-phenoxy) ethane-N,N,N',N'-tetra-acetic acid (BAPTA) in order to suppress endogenous Ca^{2+}-activated Cl^- currents, three hours prior to recording. Electrodes contained 3M KCl, and had resistances of 0.3–1 MΩ. The holding potential (V_H) was -100 mV.

Cell culture, heterologous expression and whole cell recording. The tsA-201 cells were cultured in a medium consisting of D-MEM, 10% fetal bovine serum, 2 mM glutamine, 100 IU/ml penicillin and 100 μg/ml streptomycin. The cDNAs (all at 1 μg/μl) for $Ca_v\alpha_1$ subunits, $Ca_v\beta$, $\alpha_2\delta$-2 and GFP (when used as a reporter of transfected cells) were mixed in a ratio of 3:2:2:0.4. The cells were transfected using Fugene 6 (Roche Diagnostics, Lewes, UK; DNA/Fugene 6 ratio of 2 μg in 3 μl). The tsA-201 cells were replated at low density on 35 mm tissue culture dishes on the day of recording. Whole-cell patch-clamp recordings were performed at room temperature (22–24°C). Only fluorescent cells expressing

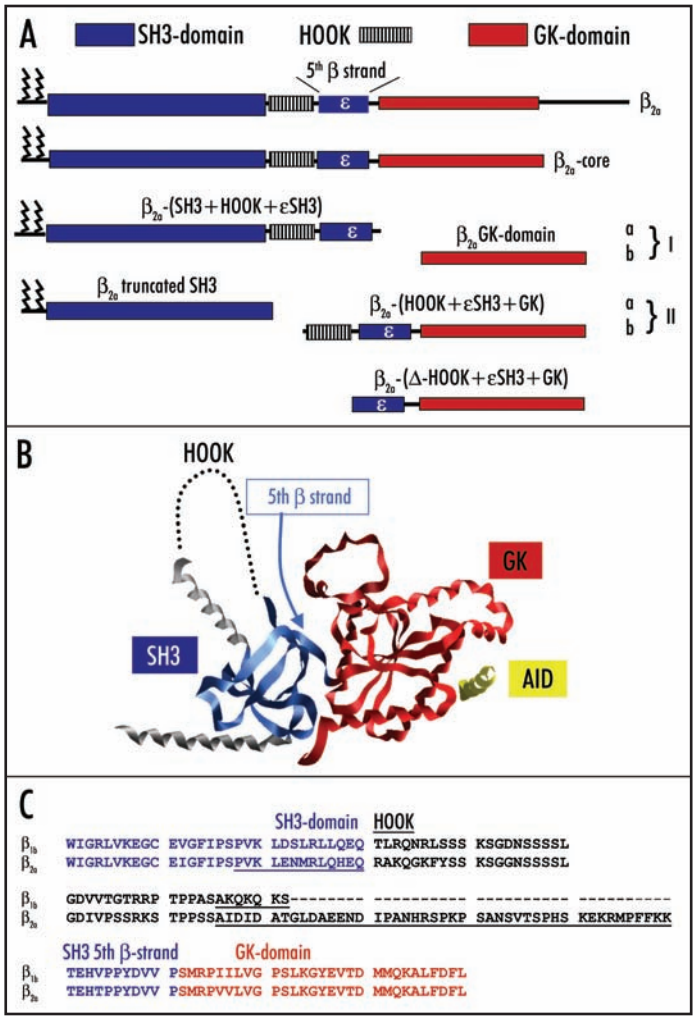

Figure 1. Constructs used in the study and alignment of the HOOK-domains of β_{2a} and β_{1b}. (A) Diagram the main constructs used in the study. Full length β_{2a} consists of an N-terminal di-palmitoylation site, the N-terminal SH3-domain (blue bar), the HOOK-domain (black striped bar), the fifth (ε) β-strand of the SH3-domain (blue bar labelled ε), the GK-domain (red bar), and a C-terminal sequence. The amino acids present in each construct are: β_{2a}-core (without the C-terminus; 1-442), β_{2a}-(SH3+HOOK+εSH3) (1–225), β_{2a}-GK (226–442), β_{2a} truncated SH3 (1–135), β_{2a}-(HOOK+εSH3+GK) (136-442); β_{2a}-(ΔHOOK+εSH3+GK) (214–442). (B) Structure of a complex between the β2-subunit of a voltage-gated Ca^{2+} channel and the α_1-interaction domain (AID, yellow helix) of the $Ca_v\alpha_1$ subunit determined by Opatowsky et al.,[12] shown as a ribbon representation, redrawn from a previous (reviewed in ref. 15). The SH3-domain is shown in blue, and the GK domain in red. The structure of the HOOK region was not determined and is here shown as a dotted line. (C) Alignment of the end of the SH3-domain (in blue), including the additional conserved helix starting PVK (underlined), the HOOK domain (black, with the variable exon underlined) and the start of the GK domain (in red), for the rat β_{1b} and β_{2a} constructs used in this study, showing the position of the HOOK sequences.

GFP were used for recording. The single cells were voltage-clamped using an Axopatch 200B patch-clamp amplifier (Molecular Devices). The electrode potential was adjusted to give zero current between pipette and external solution before the cells were attached. The cell capacitance varied from 10–40 pF. Patch pipettes were filled with a solution containing (in mM) 140 Cs-aspartate, 5 EGTA, 2 $MgCl_2$, 0.1 $CaCl_2$, 2 K_2ATP, 10 HEPES, titrated to pH 7.2 with CsOH (310 mOsm), with a resistance of 2–3 MΩ. The external solution contained (in mM) 150 tetraethylammonium (TEA) bromide, 3 KCl, 1.0 $NaHCO_3$, 1.0 $MgCl_2$, 10 HEPES, 4 glucose, 10 $BaCl_2$, pH adjusted to 7.4 with Tris-Base (320 mOsm). The pipette and cell capacitance as well as the series resistance were compensated by 80%. Leak and residual capacitance current were subtracted using a P/4 protocol. Data were filtered at 2 kHz and digitized at 5–10 kHz. The holding potential was -100 mV, and pulses were delivered every 10 seconds.

Data analysis and curve fitting. Current amplitude was measured 10 ms after the onset of the test pulse, and the average over a 2 ms period was calculated and used for subsequent analysis. The current density-voltage (*I-V*) relationships were fitted with a modified Boltzmann equation as follows:

$$I=G_{max}*(V-V_{rev})/(1+\exp(-(V-V_{50,act})/k))$$

where I is the current density (in pA/pF), G_{max} is the maximum conductance (in nS/pF), V_{rev} is the reversal potential, $V_{50,\,act}$ is the midpoint voltage for current activation, and k is the slope factor. Steady-state inactivation properties were measured by applying a 5–20 second pulse (depending on inactivation properties of the currents) from -120 to +20 mV in 10 mV increments, followed by 11 ms repolarization to -100 mV before the 100 ms test pulse to +20 mV. Steady-state inactivation and activation data were fitted with a single Boltzmann equation of the form:

$$I/I_{max}=((A1-A2)/[1+\exp((V-V_{50,inact})/k)]+A2$$

where I_{max} is the maximal current, $V_{50,inact}$ is the half-maximal voltage for current inactivation. For the steady-state inactivation, A_1 and A_2 represent the proportion of inactivating and non inactivating current, respectively. Inactivation kinetics of the currents were estimated by fitting the decaying part of the current traces with the equation:

$$I(t) = C + A^* \exp(-(t-t_o)/\tau_{inact})$$

where t_o is zero time, C the fraction of noninactivating current, A the relative amplitude of the exponential, and τ_{inact}, its time constant. Analysis was performed using Pclamp6 or 7 and Origin 7.

Data are expressed as mean ± s.e.m. of the number of replicates: *n*. Error bars indicate standard errors of multiple determinations. Statistical significance was analyzed using Student's paired or unpaired *t*-test, or by ANOVA, with Tukey's post hoc test, if multiple comparisons were made.

RESULTS

The relative roles of N-terminal palmitoylation and the variable HOOK-domain in the retardation of inactivation by $Ca_V\beta_{2a}$. $Ca_v\beta$ subunits are members of the membrane-associated guanylate-kinase-like protein family (MAGUKs).[11,21] The SH3-domain in $Ca_v\beta$ subunits is split, in that the variable loop or HOOK region (so-named in other MAGUK proteins) is intercalated before the final (5th or ε) β-strand of the SH3-domain (Fig. 1A).[12-14] In this study we wished to examine the role of this variable HOOK-domain of both β_{2a} and β_{1b} (Fig. 1B and C). We took advantage of the fact that rat β_{2a} is N-terminally palmitoylated, endowing it with the ability almost completely to remove inactivation. We were then able to examine the relative importance of mutation of the N-terminal palmitoylation motif and deletion of the HOOK region (Fig. 2). The effects of the various $Ca_v\beta$ subunit mutations were examined on $Ca_v2.2/\alpha_2\delta$-2 currents. As expected, mutation of the dicysteine palmitoylation motif to serine (C3,4S-β_{2a}) markedly increased the inactivation rate compared to wild-type β_{2a} (Fig. 2A and B). It also hyperpolarized the mid-point of the steady-state inactivation ($V_{50,inact}$) compared to wild-type β_{2a} by 42.6 mV, from -7.9 ± 1.4 mV (n = 17) to -50.5 ± 0.6 mV (n = 18, Fig. 2C). Deletion of the variable part of the HOOK region of β_{2a} (between AIDID and FFKK, called β_{2a} Δ-vHOOK, Fig. 1C) resulted in a different behavior, inducing two current components, about 50% being rapidly inactivating, with the remaining current being completely noninactivating (Fig. 2A and B). For this reason, only a partial steady-state inactivation was obtained for this construct, even when using a 20-second conditioning step, with a $V_{50,inact}$ of -47.5 ± 1.5 mV (n = 22, Fig. 2C). We then combined the two mutations in the C3,4S-β_{2a} Δ-vHOOK construct, and observed a rapidly and completely inactivating current (Fig. 2A and B). This current exhibited a strongly hyperpolarized steady-state inactivation, with a $V_{50,inact}$ of -62.4 ± 0.6 mV (n =13, Fig. 2C).

The GK-domain constructs of β_{2a} reconstitute β-subunit mediated trafficking behavior in *Xenopus* oocytes, both with and without the associated HOOK domain. In order to examine further the role of the HOOK domain, we made two pairs of $Ca_v\beta_{2a}$-GK-domain constructs by cutting the β_{2a} subunit at two different points, either before or after the HOOK plus the εSH3 strand (Fig. 1A–C), to make β_{2a}-GK [Ib] and β_{2a}-(HOOK+εSH3+GK), [IIb] (Fig. 1A).

Both the GK-domains contain the β-binding pocket, which binds the AID region (Fig. 1B),[12,13] and would therefore be expected to traffic the channels. However, the minimal GK-domain did not contain the entire region formerly designated as the β-interaction domain or BID, which was originally described as the shortest region able to enhance calcium currents.[22] It is now clear from the $Ca_v\beta$ subunit structure that whilst this region does not actually bind the AID sequence,[12-14] it must be important for the structural integrity of the GK-domain. The variable C-terminal region after the conserved GK-domain was removed from both β_{2a}-GK constructs, while retaining 10–20 amino acids after the end of the minimal GK constructs used for structural determinations, taking the GK sequence up to the exon boundary.

In *Xenopus* oocytes it was found previously that the isolated GK-domain of $Ca_v\beta3$ commencing after the final SH3 β-strand is able to reconstitute trafficking,[14] whereas this was reported not to be the case in mammalian cells.[18] Maltez et al.[17] found that although protein formed from a long β_{2a}-GK-domain, containing the SH3 fifth β-strand, enhanced $Ca_v2.1$ currents in *Xenopus* oocytes, there was an additional effect of the truncated SH3-domain protein, when coinjected with a sub-maximal amount of the GK-domain protein.

Our initial results showed that in *Xenopus* oocytes both the β_{2a}-GK-domain and β_{2a}-(HOOK+εSH3+GK)-domain were able to fulfil the role of $Ca_v\alpha_1$ trafficking to a similar extent, promoting the formation of functional channels. The peak current size was increased 8–10-fold over the currents formed by the $Ca_v2.2/\alpha_2\delta$-2 combination

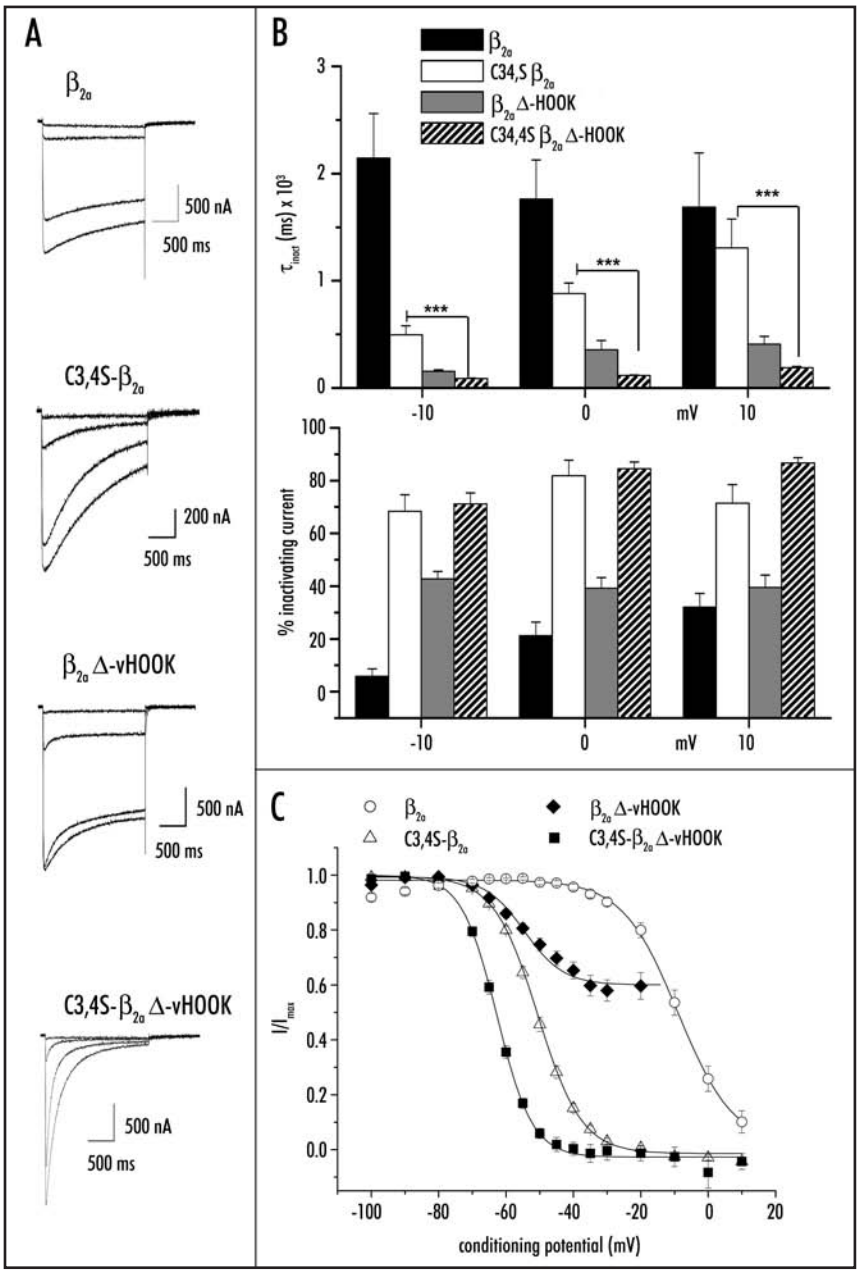

Figure 2. Relative roles of palmitoylation and the variable part of the HOOK (vHOOK) region in the retardation of inactivation mediated by β_{2a}. (A) Overlaid current traces during 2 second step depolarizations from -100 mV to -20, -10, 0 and +10 mV for β_{2a} (top), C3,4S-β_{2a} (upper middle), β_{2a} Δ-vHOOK (lower middle) and C3,4S-β_{2a} Δ-vHOOK (bottom). (B) Bar chart of τ_{inact} values (upper panel) and % of inactivating current (lower panel), for the four conditions shown in (A). β_{2a} (black bars, n = 17), C3,4S-β_{2a} (white bars, n = 13), β_{2a} Δ-vHOOK (gray bars, n = 17) and C3,4S-β_{2a} Δ-vHOOK (hatched bars, n = 16). Statistical significance of the differences between the τ_{inact} for C3,4S-β_{2a} and C3,4S-β_{2a} Δ-vHOOK are given *** $p < 0.001$. (C) Normalized steady-state inactivation for $Ca_v2.2/\alpha_2\delta$-2 with β_{2a} (open circles, n = 17), C3,4S-β_{2a} (open triangles, n = 18), β_{2a} Δ-vHOOK (closed diamonds, n = 22) and C3,4S-β_{2a} Δ-vHOOK (closed squares, n = 13). Data were fit by a Boltzmann function, and the mean parameters for the fits are given in the text and Figure 3C.

in the absence of expressed $Ca_v\beta$ subunits. The current enhancement was similar to that observed with full-length β_{2a} (Fig. 3A).

In contrast, and as previously indicated in mammalian cells,[18,23] we found that in tsA201 cells, both the β_{2a}-GK-domain and the β_{2a}-(HOOK+εSH3+GK)-domain were much less effective than full-length β_{2a} in enhancing current amplitude (Table 1), indicating that mammalian cells may have more stringent endoplasmic reticulum (ER) retention signals for the $Ca_v2.2$ α_1 subunit, or that the isolated GK-domain proteins are less stable in tsA201 cells than in oocytes. For this reason most of the subsequent studies described in this paper were performed in *Xenopus* oocytes, although comparisons were made with tsA201 cells in several instances, and these are stated in the text.

Distinctive inactivation properties of the β_{2a} GK domain when associated with the HOOK domain. In *Xenopus* oocytes, both the β_{2a}-GK-domain constructs caused a hyperpolarizing shift in the voltage-dependence of activation compared to the $Ca_v2.2/\alpha_2\delta$-2 currents in the absence of $Ca_v\beta$ subunits (Fig. 3B). In contrast to $Ca_v\beta_{2a}$, which depolarized the steady-state inactivation compared to the absence of coexpressed $Ca_v\beta$ subunits, both the free GK-domains of β_{2a} hyperpolarized the steady-state inactivation. This hyperpolarization was significantly greater for the β_{2a}-GK-domain ($V_{50,inact}$ of -55.0 mV) than for the β_{2a}-(HOOK+εSH3+GK)-domain ($V_{50,inact}$ of -45.6 mV, $p < 0.0001$; Fig. 3C and D), and was similar to the effect of the nonpalmitoylated β subunits, such as β_{1b} (Fig. 3C and D). As a control that the lack of a C-terminus was not responsible for any differences between the isolated GK-domains and full length β_{2a}, we expressed the β_{2a} core domain, which spans both these two domains, but is lacking the C-terminus (Fig. 1A). We found that this construct behaves identically to β_{2a} with regard to the parameters measured here (Fig. 3A and B, and data not shown).

In addition to its steady-state inactivation being more depolarized, the kinetics of inactivation of the β_{2a}-(HOOK+εSH3+GK)-domain were 4.3-fold slower than those of the β_{2a}-GK-domain at 0 mV (Fig. 4A and B), and similar to those of C3,4S-β_{2a} (Fig. 2A and B), again implicating the HOOK region in retarding the process of inactivation. The effect on inactivation kinetics was much more marked than the effect on closed-state inactivation. We therefore removed the HOOK sequence to form a β_{2a}-(ΔHOOK+εSH3+GK)-domain construct (Fig. 1A). The removal of the HOOK-domain resulted in a β_{2a}-GK construct with properties that were identical to the β_{2a}-GK-domain. The τ_{inact} for this construct was significantly smaller than that of the β_{2a}-(HOOK+εSH3+GK)-domain at all potentials examined (Fig. 4A and B; $p < 0.01$). Furthermore, the steady-state inactivation was also significantly hyperpolarized compared to the β_{2a}-(HOOK+εSH3+GK)-domain (Fig. 3D, $p < 0.001$), being similar to the β_{2a}-GK-domain. This confirms that it is the HOOK sequence itself that is responsible for retarding inactivation.

Very similar results were obtained in tsA201 cells, where, despite exerting a relatively small effect on trafficking, the β_{2a}-GK-domain strongly hyperpolarized the steady-state inactivation, whereas the β_{2a}-(HOOK+εSH3+GK)-domain produced less hyperpolarization (Table 1). Similarly, in tsA201 cells the kinetics of inactivation

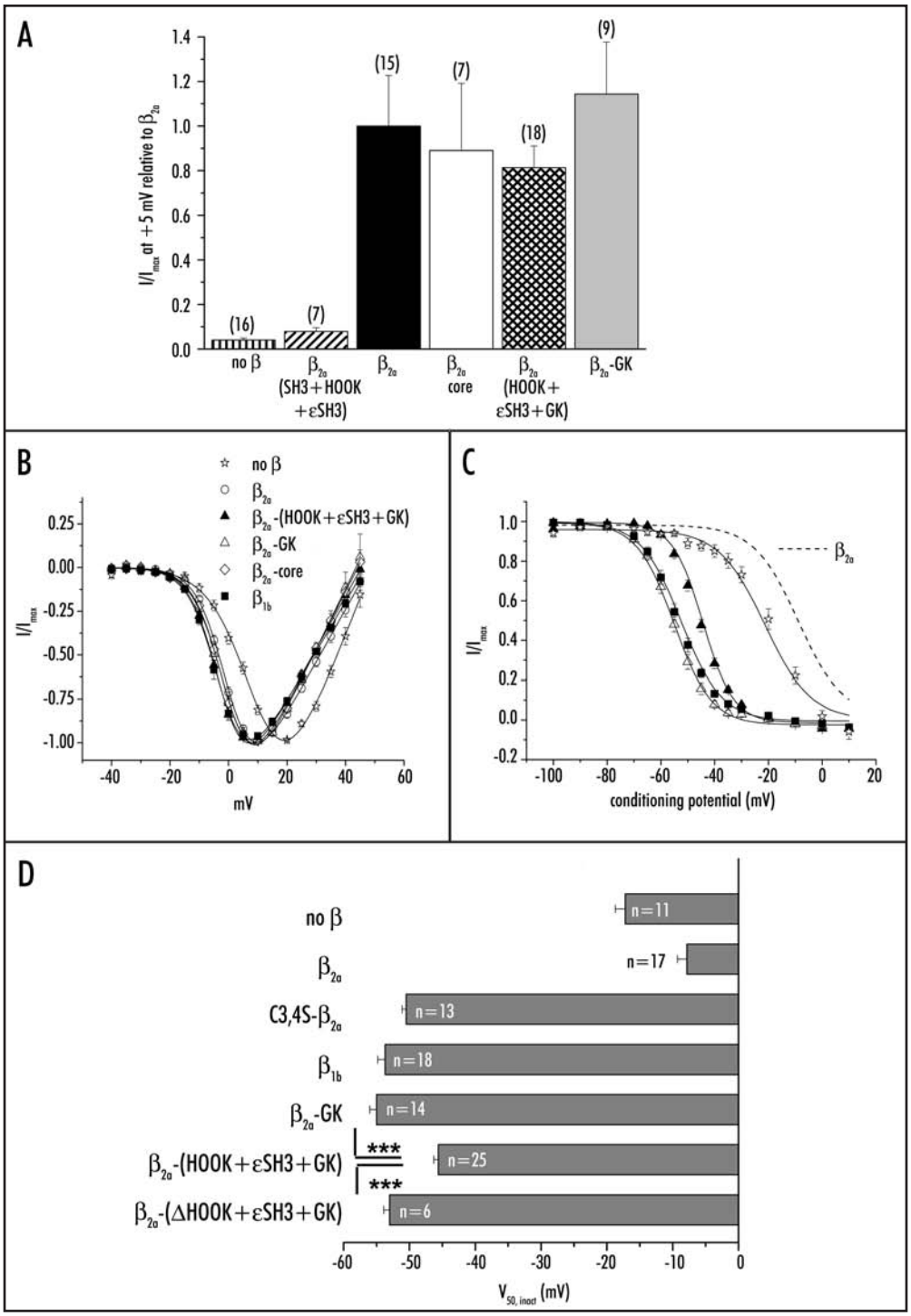

Figure 3. Current amplitude, normalized current-voltage relationships and steady-state inactivation for β_{2a}-GK-domains, compared to full length β_{2a}. (A) Current voltage-relationships were obtained for $Ca_v2.2/\alpha_2\delta$-2, without β, or together with the truncated constructs shown, and the peak current at +5 mV was normalized compared to the value for β_{2a} in each experiment. Data are without β (vertical stripes), + β_{2a}-(SH3+HOOK+εSH3) (hatched), + β_{2a} (black), + β_{2a} core (white), + β_{2a}-(HOOK+εSH3+GK) (cross-hatched) or + β_{2a}-GK (grey). The numbers of determinations are shown in parentheses. (B) Current voltage-relationships were obtained for $Ca_v2.2/\alpha_2\delta$-2, without β (open stars, n = 17; $V_{50,\ act}$ = +10.49 ± 0.96 mV), or together with the various β subunit constructs shown in the legend, and the peak current was normalized to one. β_{2a} (open circles, n = 16; $V_{50,\ act}$ = +0.41 ± 0.62 mV), β_{2a} core (open diamonds, n = 7; $V_{50,\ act}$ = -0.41 ± 0.97 mV), β_{2a}-GK (open triangles, n = 5; $V_{50,\ act}$ = +1.60 ± 0.93 mV), β_{2a}-(HOOK+εSH3+GK) (closed triangles, n = 21; $V_{50,\ act}$ = -2.41 ± 0.59 mV) and β_{1b} (closed squares, n = 13; $V_{50,\ act}$ = -2.65 ± 1.09 mV). Data were fit by a combined Boltzmann and straight line function. (C) Normalized steady-state inactivation for $Ca_v2.2/\alpha_2\delta$-2, without β (open stars, n = 12), or together with the various constructs shown: β_{2a} (dashed line, repeated from Fig. 2C), β_{2a}-GK-domain (closed triangles, n = 25), β_{2a}-(HOOK+εSH3+GK)-domain (open triangles, n = 14), and β_{1b} (closed squares, n = 18). Data were fit by a Boltzmann function, and the mean parameters for the fits are given in Figure 3D. (D) Bar chart of mean ± s.e.m. values for $V_{50,inact}$ for $Ca_v2.2/\alpha_2\delta$-2 expressed together with the β subunit constructs whose steady state inactivation is shown in Figures 2C and 3B, and also for the β_{2a}-(ΔHOOK+εSH3+GK)-domain. The number of determinations is shown on the bars. The statistical significance of the difference between the β_{2a}-(HOOK+εSH3+GK)-domain and either the β_{2a}-GK-domain alone or the β_{2a}-(ΔHOOK+εSH3+GK)-domain is indicated by *** $p < 0.0001$.

Table 1. The effect of various $Ca_v\beta$ subunit constructs on biophysical parameters of $Ca_v2.2/\alpha_2\delta$-2 calcium channel currents in tsA 201 cells

Construct $Ca_v2.2/\alpha_2\delta$-2 +	Peak amplitude (pA/pF)at +20 mV	Ratio I_{Ba}(peak)/I_{Ba} (600 ms)	$V_{50,\,act}$ (mV)	$V_{50,inact}$ (mV)
No β	-10.3 ± 2.1 (n=7)	0.24 ± 0.07 (n=10)	15.5 ± 0.1 (n=7)	-26.9 ± 0.4 (n=3)
β_{2a}	-227.6 ± 69.0 (n=8)†	0.71 ± 0.09 (n=18)†	8.5 ± 0.5 (n=8)†	-5.4 ± 1.9 (n=8)†
β_{2a}-GK	-46.4 ± 21.3 (n=7)*	0.17 ± 0.02 (n=15)*	11.1 ± 0.4 (n=7)*	-46.9 ± 0.6 (n=8)*†
β_{2a}-(HOOK+εSH3+GK)	-47.2 ± 12.9 (n=7)†*	0.30 ± 0.04 (n=14)*	9.9 ± 0.3 (n=7)†	-37.5 ± 0.4 (n=10)*†
β_{1b}	-240.8 ± 50.8 (n=15)†	0.27 ± 0.06 (n=15)	4.8 ± 0.4 (n=15)†	-41.9 ± 1.2 (n=9)†
β_{1b}-(SH3+HOOK+εSH3)	-8.7 ± 3.5 (n=8)*	0.38 ± 0.03 (n=14)	12.5 ± 0.3 (n=8)*	-28.3 ± 0.8 (n=11)*
β_{1b} trunc SH3	-7.5 ± 0.8 (n=6)*	0.30 ± 0.07 (n=6)	9.5 ± 0.9 (n=6)*	-31.5 ± 0.9 (n=3)*
β_{1b}-GK	-13.2 ± 5.3 (n=5)*	0.28 ± 0.04 (n=11)	8.4 ± 2.4 (n=5)†	-32.8 ± 1.3 (n=5)†*
β_{1b}-(HOOK+εSH3+GK)	-79.8 ± 16.2 (n=10)†*	0.08 ± 0.01 (n=10)†*	3.5 ± 0.6 (n=10)†	-48.9 ± 1.3 (n=7)†*
β_{1b}-(SH3+HOOK+εSH3) plus β_{1b}-GK	-19.0 ± 5.3 (n=12)†*	0.48 ± 0.03 (n=15)†*	12.5 ± 0.5 (n=12)†*	-32.6 ± 1 (n=5)†*
β_{1b} trunc SH3 + β_{1b}-(HOOK+εSH3+GK)	-128.2 ± 33.4 (n=11)†*	0.08 ± 0.01 (n=14)†*	3.6 ± 0.4 (n=11)†*	-56.3 ± 1.6 (n=11)†*

Statistical significances were determined for differences compared to $Ca_v2.2$ expressed without any β subunit, where† indicates $p < 0.05$; or compared to $Ca_v2.2$ expressed with the relevant wild-type β subunit counterpart, where* indicates $p < 0.05$.

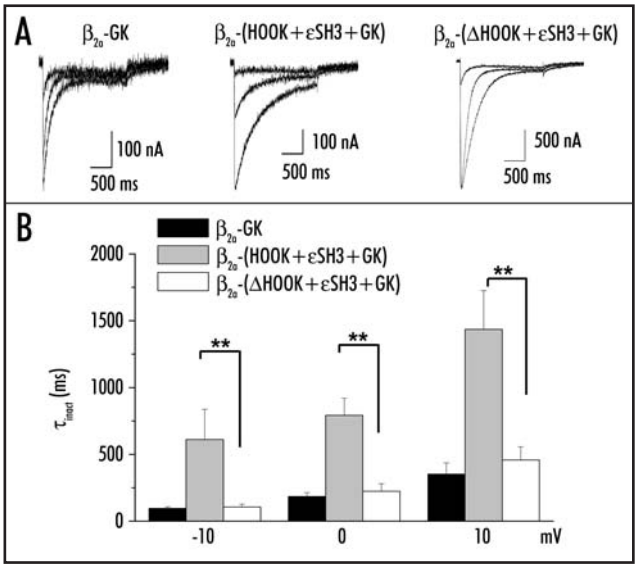

Figure 4. The kinetics of inactivation of β_{2a}-GK-domains provides evidence for a role of the HOOK-domain. (A) Families of current traces following 2 s step depolarizations from -100 mV to -10, 0 and +10 mV for β_{2a}-GK-domain alone (left), β_{2a}-(HOOK+εSH3+GK)-domain (center) and β_{2a}-(ΔHOOK+εSH3+GK)-domain (right). (B) Bar chart of τ_{inact} values (± s.e.m.) for the three conditions shown in (A). β_{2a}-GK-domain alone (black bars, n = 5), β_{2a}-(HOOK+εSH3+GK)-domain (grey bars, n = 17) and β_{2a}-(ΔHOOK+εSH3+GK)-domain (white bars, n = 5). Statistical significance of the difference between β_{2a}-(HOOK+εSH3+GK)-domain and β_{2a}-(ΔHOOK+εSH3+GK)-domain is ** $p < 0.01$.

for β_{2a}-GK-domain were accelerated compared to those of β_{2a}-(HOOK+εSH3+GK) domain (Table 1).

Demonstration of interaction between β_{2a} truncated SH3 and β_{2a}-(HOOK+εSH3+GK). To examine further the role of the HOOK-domain of β_{2a}, we used the split domain approach, which has previously been shown to be successful in restoring β subunit function.[18,23] In order to confirm the results of prior split domain studies, before further studying the role of the HOOK domain, we therefore examined the coexpression of the β_{2a}-GK domain constructs with their respective β_{2a}-SH3 domains (pairs I and II, Fig. 1A). Both of the β_{2a}-SH3-domain constructs retained the N-terminal palmitoylation motif, which has previously been shown to be responsible for the complete removal of inactivation exhibited by those β2 splice variants, including β_{2a} in which it is present.[24-27] We were therefore able to use this as an assay of whether the pairs of β_{2a}-SH3 and GK domain constructs would reconstitute this property, as this would provide evidence of interaction between the two domains.

As expected, neither of the β_{2a}-SH3-domains complimentary to the respective GK domains (constructs Ia and IIa, Fig. 1A increased the current amplitude alone, compared to the small currents observed in the absence of $Ca_v\beta$ subunits (Fig. 3A and data not shown)). For the β_{2a}-(HOOK+εSH3+GK)-domain coexpressed with the β_{2a} truncated SH3-domain, the ε-strand of the SH3-domain is expressed as part of the GK-domain construct, potentially promoting interaction between the two domains. The data in Figure 5 show that this was indeed the case, in that a combination of these two domains resulted in removal of inactivation, almost to the same extent as wild-type β_{2a} (Fig. 5A and B). Furthermore, the steady-state inactivation was very substantially depolarized compared to the β_{2a}-(HOOK+εSH3 +GK)-domain alone (Fig. 6A and B). The steady-state inactivation curve was best fit by a combination of two Boltzmann functions, with the larger component (~82%) having a $V_{50,inact}$ similar to wild-type β_{2a}, and a minor component with a $V_{50,inact}$ similar to the β_{2a}-(HOOK+εSH3+GK)-domain (Fig. 6B), suggesting either that not all the β_{2a}-(HOOK+εSH3+GK)-domain is associated with palmitoylated β_{2a} truncated SH3-domain, or that a minor fraction of this SH3-domain is not palmitoylated.

In contrast, coexpression of the β_{2a}-(SH3+HOOK+εSH3)-domain with the corresponding β_{2a}-GK-domain had no effect on the kinetic (Fig. 5A and B) or voltage-dependent (Fig. 6A and B) properties of the current formed by the combination of $Ca_v2.2/\alpha_2\delta$-2 with the β_{2a}-GK-domain alone, providing no evidence of interaction between these two intact $Ca_v\beta$ domains. In agreement with this conclusion, the kinetics of inactivation for β_{2a}-(SH3+HOOK+εSH3)-domain plus β_{2a}-GK-domain were not significantly slower than those of β_{2a}-GK-domain alone (Fig. 5B, compared to Fig. 4B), and both were much more rapid than those of β_{2a} itself.

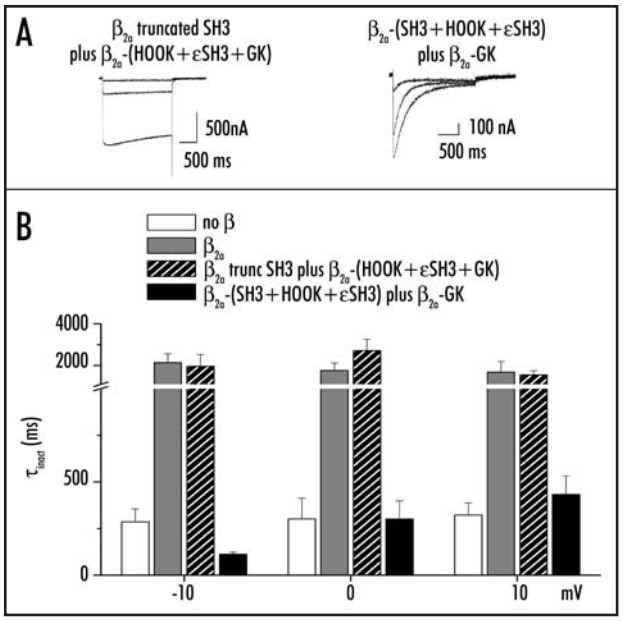

Figure 5. Only one of the two pairs of β2a SH3- and GK-domains mimics the kinetics of inactivation of β_{2a}. (A) Example traces showing inactivation kinetics for 2-second depolarizing steps to -10, 0 and +10 mV from -100 mV, for the β_{2a} truncated SH3-domain together with the β_{2a}-(HOOK+εSH3+GK)-domain (left), or the β_{2a}-(SH3+HOOK+εSH3)-domain together with the β_{2a}-GK-domain (right). (B) Time constants of inactivation obtained by fitting a single exponential to the inactivating phase of the 2 s steps, for the constructs indicated, for no β (white bars, n = 3), β_{2a} (grey bars, n = 8, obtained in parallel experiments), β_{2a} truncated SH3-domain together with the β_{2a}-(HOOK+εSH3+GK)-domain (black hatched bars, n = 7) or the β_{2a}-(SH3+HOOK+εSH3)-domain together with the β_{2a}-GK-domain (black bars, n = 3).

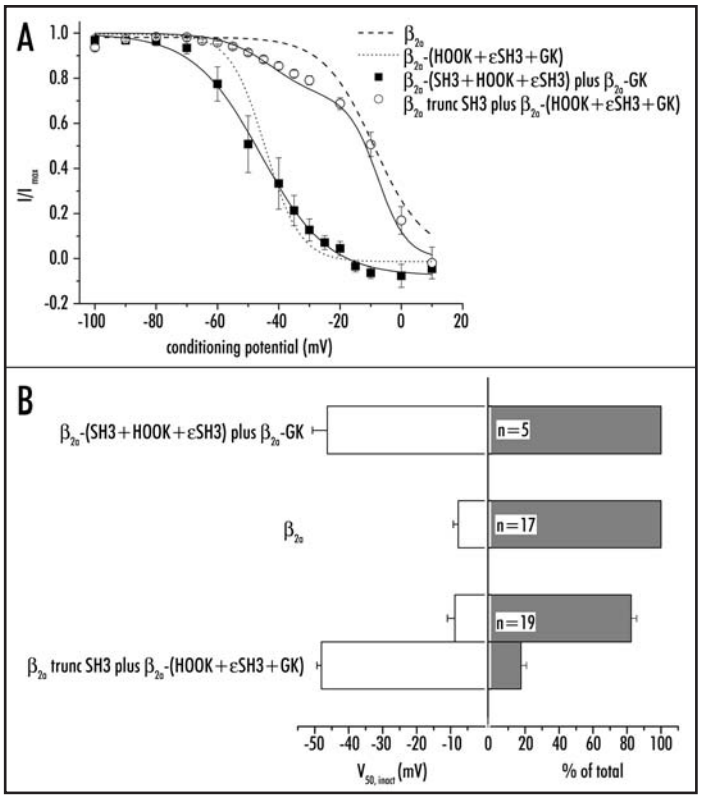

Figure 6. Only one of the two pairs of β_{2a} SH3- and GK-domains mimics the distinctive steady-state inactivation of β_{2a}. (A) Normalized steady-state inactivation curves for $Ca_v2.2/\alpha_2\delta$-2, together with the constructs shown. β_{2a} (dashed line, repeated from Fig. 2C, β_{2a}-(SH3+HOOK+εSH3)-domain (dotted line, repeated from Fig. 3C, β_{2a}-(SH3+HOOK+εSH3)-domain together with the β_{2a}-GK-domain (closed squares, n = 5) or β_{2a} truncated SH3-domain plus β_{2a}-(SH3+HOOK+εSH3)-domain (open circles, n = 17). Data were fit by single Boltzmann functions, except for the β_{2a} truncated SH3-domain together with the β_{2a}-(HOOK+εSH3+GK)-domain data, which was fit by a double Boltzmann function. The mean parameters for individual fitted data curves are given in Figure 6B. (B) Bar chart of mean ± s.e.m. values for $V_{50,inact}$ (white bars, left) and % of the total of each component (grey bars, right) for $Ca_v2.2/\alpha_2\delta$-2 expressed together with the β subunit constructs stated. The number of determinations is shown on the bars. For β_{2a} truncated SH3-domain plus β_{2a}-(SH3+HOOK+εSH3)-domain, the, the data were fit by a double Boltzmann function, and the mean ± s.e.m. given for both components.

The relative roles of the β_{2a} palmitoylated SH3-domain and the β_{2a} HOOK-domain in removal of inactivation involving the β_{2a}-GK-domain. There are three nonexclusive mechanisms that may be responsible for the removal of inactivation when the β_{2a}-(HOOK+εSH3+GK)-domain and the β_{2a} truncated SH3-domain are coexpressed. Firstly, it is likely that the presence of the palmitoylation on the SH3-domain reduces inactivation by anchoring the GK-domain and its associated I-II linker. This requires that the two domains interact. Secondly, it may be that their interaction then promotes a change in conformation of the GK-domain. Thirdly, there appears to be a role for a specific motif in the β_{2a} HOOK-domain in retarding inactivation. The involvement of the β_{2a} HOOK region is suggested by the fact that the β_{2a}-(HOOK+εSH3+GK)-domain shows a four-fold slowing of inactivation kinetics, and a steady-state inactivation that is significantly more depolarized than the short β_{2a}-GK-domain (Figs. 3C and D and 4A and B), and by the finding that deletion of the variable region of the HOOK-domain of β_{2a} results in a rapidly inactivating current component (Fig. 2).

We then wished to determine whether the demonstrated interaction between the β_{2a} truncated SH3-domain and the β_{2a}-(HOOK+εSH3+GK)-domain was important, for example to present the HOOK region in a correct orientation, by using the truncated SH3-domain from β_{1b}, which is not palmitoylated. We first examined the effect of the β_{1b} truncated SH3-domain on the β_{1b}-(HOOK+εSH3+GK)-domain. Their coexpression resulted in currents with a steady-state inactivation that was hyperpolarized to a similar extent to β_{1b} itself, and was also similar to either of the β_{1b} GK-domains alone (Fig. 7A and B). In tsA201 cells, similar results were observed for the combination of the β_{1b} truncated SH3-domain and β_{1b}-(HOOK+εSH3+GK)-domain (Table 1). In contrast, in this expression system, there was little evidence that the short β_{1b} GK-domain, either alone or in combination, had any influence to enhance current amplitude, or on other parameters of activation or inactivation (Table 1).

In *Xenopus* oocytes, we observed comparable hyperpolarization of the steady-state inactivation with the combination of the β_{1b} truncated SH3-domain and either β_{1b} (HOOK+εSH3+GK)-domain or β_{1b}-(ΔHOOK+εSH3+GK)-domain (Fig. 7B). In contrast, when the β_{1b} truncated SH3-domain was coexpressed with the β_{2a}-(HOOK+εSH3+GK)-domain, this combination significantly shifted the steady-state inactivation to more positive potentials (Fig. 7A and B). This effect was lost if the HOOK sequence was removed to form the β_{2a}-(ΔHOOK+εSH3+GK)-domain. Using this construct together with β_{1b} truncated SH3 domain, the steady-state

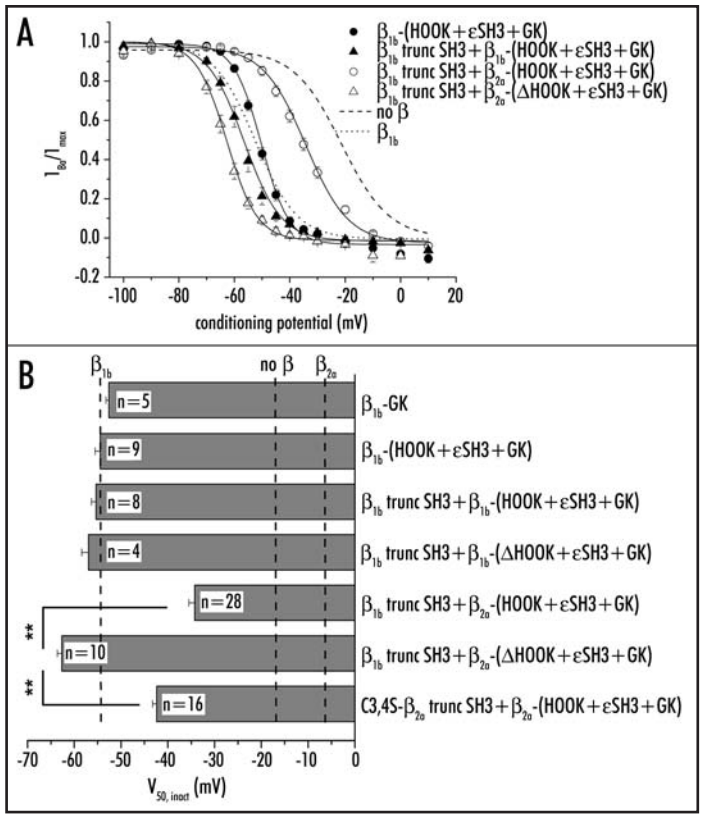

Figure 7. Steady-state inactivation for combinations of β-subunit constructs, showing the role of the β_{2a} HOOK-domain. (A) Normalized steady-state inactivation curves for $Ca_v2.2/\alpha_2\delta$-2, together with the constructs shown. No β (dashed line, repeated from Fig. 3C, β_{1b} (dotted line, repeated from (Fig. 3C), β_{1b}-(HOOK+εSH3+GK)-domain (closed circles, n = 9), β_{1b} truncated SH3-domain plus β_{1b}-(HOOK+εSH3+GK)-domain (closed triangles, n = 8), β_{1b} truncated SH3-domain plus β_{2a}-(HOOK+εSH3+GK)-domain (open circles, n = 28) and β_{1b} truncated SH3-domain plus β_{2a}-(ΔHOOK+εSH3+GK)-domain (open triangles, n = 10). Data were fit by single Boltzmann function, and the mean parameters for individual fitted data curves are given in Figure 7B. (B) Bar chart of $V_{50,inact}$ for $Ca_v2.2/\alpha_2\delta$-2 expressed together with the β subunit constructs stated. The number of determinations is shown on the bars. The statistical significances of the differences are indicated by ** $p < 0.01$. The $V_{50,inact}$ values for $+\beta_{2a}$, $+\beta_{1b}$ and without β are indicated for comparison by dashed vertical lines.

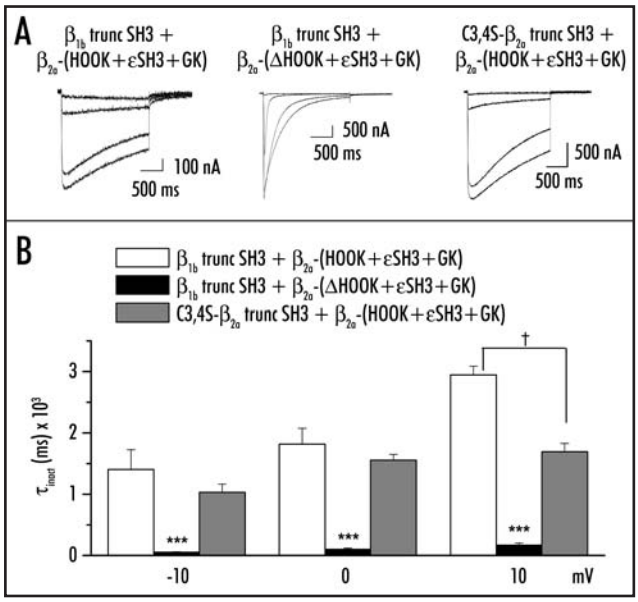

Figure 8. Kinetics of inactivation for combinations of β_{2a} and β_{1b} truncated SH3-domain with the β_{2a}-(HOOK+εSH3+GK)-domain in the presence or absence of the HOOK-domain or palmitoylation motif. (A) Example traces showing inactivation kinetics for 2 s depolarizing steps to -20, -10, 0 and +10 mV from -100 mV, for β_{1b} truncated SH3-domain together with β_{2a}-(HOOK+εSH3+GK)-domain (left), β_{1b} truncated SH3-domain together with β_{2a}-(ΔHOOK+εSH3+GK)-domain (centre) and C3,4S-β_{2a} truncated SH3-domain together with β_{2a}-(HOOK+εSH3+GK)-domain (right). (B) Bar chart of time constants of inactivation obtained by fitting a single exponential to the inactivating phase of the 2-second steps, for β_{1b} truncated SH3-domain together with β_{2a}-(HOOK+εSH3+GK)-domain (white bars, n = 10), β_{1b} truncated SH3-domain together with β_{2a}-(ΔHOOK+εSH3+GK)-domain (black bars, n = 12) and C3,4S-β_{2a} truncated SH3-domain together with β_{2a}-(HOOK+εSH3+GK)-domain (grey bars, n = 9). Statistical significance of the differences between β_{1b} truncated SH3-domain together with β_{2a}-(ΔHOOK+εSH3+GK)-domain and the other conditions are given by *** $p < 0.001$, and between β_{1b} truncated SH3-domain together with β_{2a}-(HOOK+εSH3+GK)-domain and C3,4S-β_{2a} truncated SH3-domain together with β_{2a}-(HOOK+εSH3+GK)-domain at +10 mV† $p < 0.05$.

inactivation was strongly hyperpolarized, to a similar extent to a combination with any of the β_{1b} GK-domain constructs (Fig. 7A and B). Similarly, the kinetics of inactivation were much more rapid for the combination of the β_{1b} truncated SH3-domain with the β_{2a}-(ΔHOOK+εSH3+GK)-domain, than with the β_{2a}-(HOOK+εSH3+GK)-domain (Fig. 8A and B).

It is evident that any combination containing the β_{2a}-(HOOK+εSH3+GK)-domain results in a slower inactivation rate and a decrease in the extent to which the voltage-dependence of inactivation is hyperpolarized. This specifically requires the presence of the HOOK-domain of β_{2a}. Thus, despite the absence of the palmitoylation motif on the β_{1b} truncated SH3-domain, the presence of other attributes, in particular the unique HOOK sequence contributed by the β_{2a}-(HOOK+εSH3+GK)-domain contributes to the removal of inactivation. The combination of the nonpalmitoylatable C3,4S-β_{2a}-SH3-domain with the β_{2a}-(HOOK+εSH3+GK)-domain resulted in a $V_{50,inact}$ for steady-state inactivation similar to that for the β_{1b} truncated SH3-domain and β_{2a}-(HOOK+εSH3+GK)-domain (Fig. 7B). It also showed similar inactivation kinetics, which were much slower than in the absence of the HOOK domain (Fig. 8A and B).

DISCUSSION

Requirement of $Ca_V\beta$ GK-domains for plasma membrane expression of HVA calcium channels. One of the main effects of $Ca_v\beta$ subunits on HVA calcium channels is to increase current density. However, the mechanism for this increase remains controversial, either being attributed to increased trafficking,[6] increased maximum open probability[29] or both. In agreement with the first hypothesis, we and others have shown biochemically that the amount of $Ca_v\alpha_1$ subunits in the plasma membrane is increased by $Ca_v\beta$ subunits.[10,30,31] This finding was reinforced by the fact that fewer channels were present at the surface when the mutated $Ca_v2.2$W391A channels, that did not interact with β subunits, were cotransfected with a $Ca_v\beta$.[10] It has been suggested that when a $Ca_v\beta$ subunit is bound to the I-II linker, it may mask an ER retention signal present in the I-II linker of HVA calcium channels and favor the trafficking of the channel to the cell surface,[6] although no specific ER retention signal has been identified. All of the free GK-domains of β_{1b} and β_{2a} tested here

produced an enhancement of current density in *Xenopus* oocytes in a manner largely indistinguishable from full-length $Ca_v\beta$ subunits, whereas in tsA201 cells the effect on current amplitude was reduced, compared to full length β_{2a} or β_{1b}, particularly for the minimal GK domains. This suggests that the processes limiting plasma membrane expression of $Ca_v\alpha_1$ subunits are to some extent dependent on the expression system used, or they may depend on differences in the stability or folding of the expressed domains in the different systems. Oocytes are incubated at 17–18°C, whereas mammalian cells are maintained at 37°C, and lower temperatures are known to reduce protein mis-folding. The GK domains used in the present study terminated at the exon boundary, marking the end of the second conserved domain, as this was most likely to delineate a domain that would be stable to proteolysis.

Determinants of inactivation: Role of the $Ca_V\alpha_1$ I-II linker. In the absence of any expressed $Ca_v\beta$ subunits, the steady-state inactivation of $Ca_v2.2$ was relatively depolarized, with a mid-point at about -15 mV in *Xenopus* oocytes in 10 mM Ba^{2+}. The $V_{50,inact}$ was hyperpolarized by all $Ca_v\beta$ subunits, except palmitoylated β_{2a}. In the present study β_{1b} produced a negative shift (of -27 mV), compared to the absence of coexpressed $Ca_v\beta$ subunits. Here we have shown that steady-state inactivation was hyperpolarized by the presence of any of the free GK-domains of β_{1b} and β_{2a}. This suggests that the binding of the GK-domain itself to the AID initiates the processes involved in inactivation. This is in agreement with the finding that mutation of the AID amino acids is also able to modify inactivation.[10,32] It has been suggested that binding of the GK-domain to the AID sequence may induce the residues in the I-II linker proximal to the AID to form a rigid α-helix, and that this is involved in initiating inactivation.

Determinants of inactivation: Role of the HOOK-domain and potential interaction with β_{2a} palmitoylation. This study provides several main pieces of evidence that the HOOK domain is involved in regulating the process of inactivation. Firstly, the difference between β_{2a}-(HOOK+εSH3+GK) domain compared to β_{2a}-GK alone is a depolarisation of the steady state inactivation by 10 mV and ~4-fold slowing of inactivation kinetics. Secondly, the difference between C3,4S-β_{2a} compared to C3,4S-β_{2a}(Δ-vHOOK) is a 12 mV shift of steady-state inactivation and ~7-fold slowing of the inactivation kinetics. Thirdly, the difference between β_{2a}-(HOOK+εSH3+GK) + β_{1b} truncSH3, compared to β_{2a}-(ΔHOOK+εSH3+GK) + either β_{1b} truncSH3 or C3,4S-β_{2a} truncSH3 is ~20 mV shift of the steady-state inactivation and ~15-fold slowing of the inactivation kinetics.

Further removal of inactivation is promoted by coexpressing the palmitoylated β_{2a} truncated SH3-domain with the β_{2a}-(HOOK+εSH3+GK)-domain, to a value approaching that for β_{2a} itself. It is possible that this interaction allows presentation of the β_{2a} HOOK-domain in the correct orientation to slow the kinetics of inactivation and depolarize steady-state inactivation.

Taken together, these results all point to the importance of the HOOK region of β_{2a} in the retarding inactivation. They also point to the possibility that palmitoylation of β_{2a}, resulting in a much higher concentration beneath the plasma membrane, may allow stable docking of the β_{2a} HOOK-domain with a potential binding site on the α_1 subunit.

Role of specific residues in the HOOK-domain. The HOOK-domain of all β subunits is involved in alternative splicing and contains either a long exon (AIDIDATGLDAEENDIPANHRS PKPSANSVTSPHSKEKRMPFFKK, 45 residues in β2) present in all the relevant β_{2a} constructs used in this study (Fig. 1A), or a short exon (AKQKQKS in β_{1b}), present in all the relevant β_{1b} construct used here (Fig. 1A). A possible role for this variable region of β subunits in inactivation was first suggested prior to any structural studies.[33] It will be of interest in the future to mutate specific residues in these HOOK regions.

Role of the $Ca_V\beta$ SH3-domain. It was shown recently that short $Ca_v\beta$ subunits lacking the GK-domain retain the ability to modulate the open probability of $Ca_v1.2$, suggesting another low affinity binding site on the Ca_v subunit for the SH3-domain.[31] An interaction between the β2 SH3-domain and the I-II linker has recently been demonstrated, that modulates biophysical properties of calcium channels, including their inactivation.[17] The authors suggested that the role of the high affinity GK-AID interaction is to increase the local concentration of $Ca_v\beta$ and to promote lower affinity interactions that occur on the I-II linker via the SH3 subunit. However, in a recent study we did not find any interaction of $Ca_v\beta_{1b}$ with the full length $Ca_v2.2$ I-II linker containing a mutation (W391A) that abrogates interaction with the AID motif; thus we have found no evidence for a second low affinity site on the I-II linker of this channel, at least one that can be observed using Biacore methodology.[34] Furthermore, the measured affinities of β_{1b} for the full length I-II linker and the I-II linker truncated just after the AID were identical.[10,34] An important role of the SH3 domain may therefore be to bind to the GK domain, thus orienting the HOOK domain correctly.

CONCLUSION

Our results indicate that two processes are occurring to retard inactivation. Firstly if palmitoylation is present, it tethers the $Ca_v\beta$ subunit to the membrane and enhances its local concentration, ensuring the AID region is always occupied by a β subunit. Potentially this palmitoylation also restricts the movement of the I-II linker via its binding to the $Ca_v\beta_{2a}$-GK-domain, and prevents it from instigating inactivation.[35,36] Secondly, residues in the HOOK-domain, particularly of β2, act in a concerted manner to retard the inactivation processes. It was shown previously using mutated β2 subunits, where the SH3 and GK domains were separately mutated so that they did not interact intramolecularly, that it was possibly to obtain interaction in trans, restoring the very slow inactivation seen with intact plamitoylated β2.[21] Our results suggest that palmitoylation of the SH3-domain is likely to ensure that the HOOK sequence is present at high concentration and able to associate with its binding site on the α_1 subunit. Whilst it is possible that the HOOK-domain enhances the interaction between the β_{2a}-SH3 and GK-domains or interacts with part of the GK domain, the fact that the β_{2a}-(HOOK+εSH3+GK)-domain showed a significantly more depolarized steady-state inactivation and much slower inactivation kinetics than the β_{2a}-GK-domain suggests the HOOK domain has a direct role in retarding inactivation possibly by interaction with the calcium channel α_1 subunit itself.

References

1. Ertel EA, Campbell KP, Harpold MM, Hofmann F, Mori Y, Perez-Reyes E, Schwartz A, Snutch TP, Tanabe T, Birnbaumer L, Tsien RW, Catterall WA. Nomenclature of voltage-gated calcium channels. Neuron 2000; 25:533-35.
2. Catterall WA. Structure and regulation of voltage-gated Ca^{2+} channels. Annu Rev Cell Dev Biol 2000; 16:521-55.
3. Dolphin AC. β subunits of voltage-gated calcium channels. J Bioeng. Biomemb 2003; 35:599-620.
4. Pragnell M, De Waard M, Mori Y, Tanabe T, Snutch TP, Campbell KP. Calcium channel β-subunit binds to a conserved motif in the I-II cytoplasmic linker of the α_1-subunit. Nature 1994; 368:67-70.
5. Brice NL, Berrow NS, Campbell V, Page KM, Brickley K, Tedder I, Dolphin AC. Importance of the different β subunits in the membrane expression of the α_{1A} and α_2 calcium channel subunits: Studies using a depolarisation-sensitive α_{1A} antibody. Eur J Neurosci 1997; 9:749-59.

6. Bichet D, Cornet V, Geib S, Carlier E, Volsen S, Hoshi T, Mori Y, De Waard M. The I-II loop of the Ca^{2+} channel α_1 subunit contains an endoplasmic reticulum retention signal antagonized by the β subunit. Neuron 2000; 25:177-90.
7. Canti C, Davies A, Berrow NS, Butcher AJ, Page KM, Dolphin AC. Evidence for two concentration-dependent processes for β subunit effects on α_{1B} calcium channels. Biophys J 2001; 81:1439-1451.
8. Walker D, Bichet D, Campbell KP, De Waard M. A β_4 isoform-specific interaction site in the carboxyl-terminal region of the voltage-dependent Ca^{2+} channel α_{1A} subunit. J Biol Chem 1998; 273:2361-7.
9. Stephens GJ, Page KM, Bogdanov Y, Dolphin AC. The α_{1B} calcium channel amino terminus contributes determinants for β subunit mediated voltage-dependent inactivation properties. Journal of Physiology 2000; 525:377-90.
10. Leroy J, Richards MS, Butcher AJ, Nieto-Rostro M, Pratt WS, Davies A, Dolphin AC. Interaction via a key tryptophan in the I-II linker of N-type calcium channels is required for β1 but not for palmitoylated β2, implicating an additional binding site in the regulation of channel voltage-dependent properties. J Neurosci 2005; 25:6984-96.
11. Hanlon MR, Berrow NS, Dolphin AC, Wallace BA. Modelling of a voltage-dependent Ca^{2+} channel β subunit as a basis for understanding its functional properties. FEBS Lett 1999; 445:366-70.
12. Opatowsky Y, Chen CC, Campbell KP, Hirsch JA. Structural analysis of the voltage-dependent calcium channel β subunit functional core and its complex with the α_1 interaction domain. Neuron 2004; 42:387-99.
13. Van Petegem F, Clark KA, Chatelain FC, Minor Jr DL. Structure of a complex between a voltage-gated calcium channel β-subunit and an α-subunit domain. Nature 2004; 429:671-5.
14. Chen YH, Li MH, Zhang Y, He LL, Yamada Y, Fitzmaurice A, Shen Y, Zhang H, Tong L, Yang J. Structural basis of the α_1-β subunit interaction of voltage-gated Ca^{2+} channels. Nature 2004; 429:675-80.
15. Richards MW, Butcher AJ, Dolphin AC. Calcium channel α subunits: Structural insights AID our understanding. TiPS 2004; 25:626-32.
16. Birnbaumer L, Qin N, Olcese R, Tarteilus E, Platano E, Costantin J, Stefani E. Structures and functions of calcium channel β subunits. J Bioeng Biomemb 1998; 30:357-76.
17. Maltez JM, Nunziato DA, Kim J, Pitt GS. Essential $Ca_v\beta$ modulatory properties are AID-independent. Nat Struct Mol Biol 2005; 12:372-7.
18. Takahashi SX, Miriyala J, Colecraft HM. Membrane-associated guanylate kinase-like properties of β-subunits required for modulation of voltage-dependent Ca^{2+} channels. Proc Natl Acad Sci USA 2004; 101:7193-8.
19. Barclay J, Balaguero N, Mione M, Ackerman SL, Letts VA, Brodbeck J, Canti C, Meir A, Page KM, Kusumi K, Perez-Reyes E, Lander ES, Frankel WN, Gardiner RM, Dolphin AC, Rees M. Ducky mouse phenotype of epilepsy and ataxia is associated with mutations in the *Cacna2d2* gene and decreased calcium channel current in cerebellar Purkinje cells. J Neurosci 2001; 21:6095-104.
20. Canti C, Page KM, Stephens GJ, Dolphin AC. Identification of residues in the N-terminus of α_{1B} critical for inhibition of the voltage-dependent calcium channel by Gβγ. J Neurosci 1999; 19:6855-64.
21. Mcgee AW, Nunziato DA, Maltez JM, Prehoda KE, Pitt GS, Bredt DS. Calcium channel function regulated by the SH3-GK module in β subunits. Neuron 2004; 42:89-99.
22. De Waard M, Pragnell M, Campbell KP. Ca^{2+} channel regulation by a conserved β subunit domain. Neuron 1994; 13:495-503.
23. Takahashi SX, Miriyala J, Tay LH, Yue DT, Colecraft HM. A $Ca_V\beta$ SH3/guanylate kinase domain interaction regulates multiple properties of voltage-gated Ca^{2+} channels. J Gen Physiol 2005; 126:365-77.
24. Qin N, Platano D, Olcese R, Costantin JL, Stefani E, Birnbaumer L. Unique regulatory properties of the type 2a Ca^{2+} channel β subunit caused by palmitoylation. Proc Natl Acad Sci USA 1998; 95:4690-5.
25. Chien AJ, Carr KM, Shirokov RE, Rios E, Hosey MM. Identification of palmitoylation sites within the L type calcium channel β_{2a} subunit, and effects on channel function. J Biol Chem 1996; 271:26465-9.
26. Bogdanov Y, Brice NL, Canti C, Page KM, Li M, Volsen SG, Dolphin AC. Acidic motif responsible for plasma membrane association of the voltage-dependent calcium channel β_{1b} subunit. Eur J Neurosci 2000; 12:894-902.
27. Takahashi SX, Mittman S, Colecraft HM. Distinctive modulatory effects of five human auxiliary β2 subunit splice variants on L type calcium channel gating. Biophys J 2003; 84:3007-21.
28. Berrou L, Klein H, Bernatchez G, Parent L. A specific tryptophan in the I-II linker is a key determinant of β- subunit binding and modulation in $Ca_v2.3$ calcium channels. Biophys J 2002; 83:1429-42.
29. Neely A, Garcia-Olivares J, Voswinkel S, Horstkott H, Hidalgo P. Folding of active calcium channel β_{1b}-subunit by size-exclusion chromatography and its role on channel function. J Biol Chem 2004; 279:21689-94.
30. Altier C, Dubel SJ, Barrère C, Jarvis SE, Stotz SC, Spaetgens RL, Scott JD, Cornet V, De Waard M, Zamponi GW, Nargeot J, Bourinet E. Trafficking of L-type calcium channels mediated by the postsynaptic scaffolding protein AKAP79. J Biol Chem 2002; 277:33598-603.
31. Cohen RM, Foell JD, Balijepalli RC, Shah V, Hell JW, Kamp TJ. Unique modulation of L-type Ca^{2+} channels by short auxiliary β_{1d} subunit present in cardiac muscle. Am J Physiol Heart Circ Physiol 2005; 288:H2363-74.
32. Herlitze S, Hockerman GH, Scheuer T, Catterall WA. Molecular determinants of inactivation and G protein modulation in the intracellular loop connecting domains I and II of the calcium channel α_{1A} subunit. Proc Natl Acad Sci USA 1997; 94:1512-6.
33. Qin N, Olcese R, Zhou JM, Cabello OA, Birnbaumer L, Stefani E. Identification of a second region of the β-subunit involved in regulation of calcium channel inactivation. Am J Physiol Cell Physiol 1996; 271:C1539-45.
34. Butcher AJ, Leroy J, Richards MW, Pratt WS, Dolphin AC. The importance of occupancy rather than affinity of CaV{β} subunits for the calcium channel I-II linker in relation to calcium channel function. J Physiol 2006; 574:387-98.
35. Restituito S, Cens T, Barrere C, Geib S, Galas S, De Waard M, Charnet P. The β_{2a} subunit is a molecular groom for the Ca^{2+} channel inactivation gate. J Neurosci 2000; 20:9046-52.
36. Stotz SC, Hamid J, Spaetgens RL, Jarvis SE, Zamponi GW. Fast inactivation of voltage-dependent calcium channels - A hinged-lid mechanism? J Biol Chem 2000; 275:24575-82.